DRFC/CAD EUR-CEA-FC-1490

# A NEW DETECTION METHOD USED TO CALIBRATE FABRY PEROT INTERFEROMETERS IN THE INFRARED RANGE

M. TALVARD, C. JAVON, M. GARCIN, D. THOUVENIN

June 1993

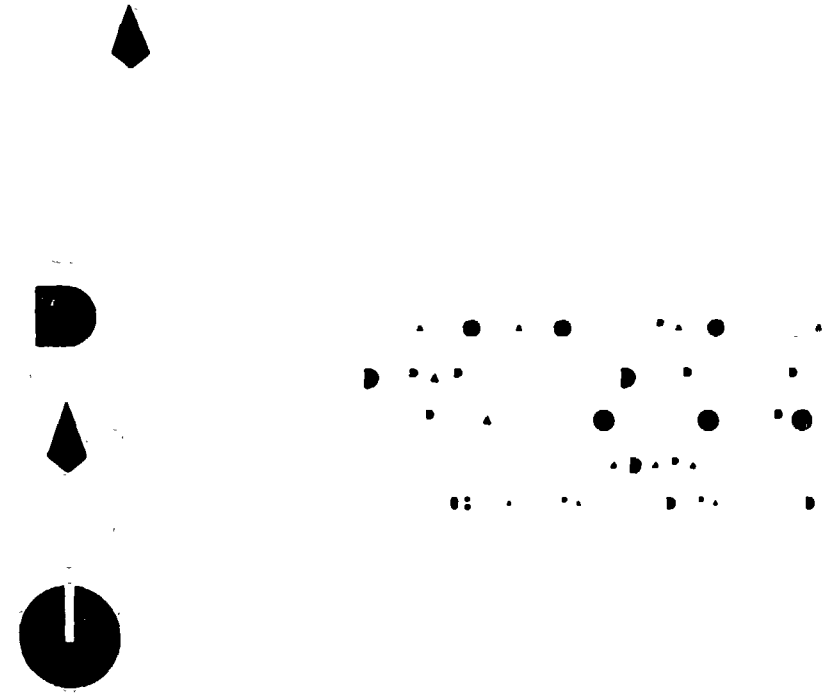

# A new detection method used to calibrate Fabry-Perot interferometers in the infrared range

**M.Talvard, C.Javon, M.Garcin, D.Thouvenin**

*Association Euratom-CEA sur la Fusion*
*Centre d'Etude de Cadarache*
*13108 Saint Paul-lez-Durance (FRANCE)*

**abstract :** Fabry-Perot interferometers are routinely used in the Tore Supra tokamak in order to measure the time evolution of the electron temperature of the confined plasmas. Calibration of such interferometers requires the detection of very low DC levels (0.1 nV) with signal-to-noise ratios less than $10^{-5}$, which is generally not compatible with standard detection methods. A new correlation method to achieve this absolute calibration is proposed. It is based on a proper noise auto-correlation technique combined with an optimized signal filtering involving Fourier analysis. The advantages of the method are detailed and experimentally compared to standard averaging techniques, such as coherent addition and synchronous detection. The method can be used in a more general context every time very small amplitude signals are to be measured.

## I. INTRODUCTION

Since the beginning of the century, Fabry-Perot interferometers have been extensively employed mainly in atomic physics, astronomy, astrophysics and light scattering. Over the past twenty years, several applications have been developed in the new areas of modern physics such as velocimetry, optical bistability or infrared spectroscopy [1]. The latter area has in particular been widely studied in the 100-1000 GHz frequency range (sub-millimetric wavelength) [2]. This corresponds to measurements of pure rotational spectra of light molecules, absorption band in solids and liquids and more directly related to the work presented here : measurements of electron cyclotron emission ( ECE ) in magnetically confined plasmas.

In the millimetric region, highly reflecting plates of Fabry-Perot cavities are composed of electroformed metal meshes [3]. In particular for tokamaks applications, Fabry-Perot interferometers have been developed to measure the plasma electron cyclotron emission spectrum especially in the optically thick region for which the intensity $I(\omega)$ is directly proportional to the local electron temperature $T_e(R)$ at the frequency dependent radius $R(\omega)$ [4,5,6]. Both good finesse of cavities ( $\approx 50$ ) and excellent time response of InSb detectors used at these frequencies provide space and time resolved $T_e$ measurements in the plasma.

In order to obtain the electron temperature, a calibration of the spectral measurements is necessary. In practice, one has to determine the calibration curve $C(\omega)$ defined as :

$$T_e(R(\omega)) = \frac{I(\omega)}{C(\omega)} \qquad (\text{keV}),$$

where $I(\omega)$ is the response in millivolts in presence of a plasma.

Calibration of Fabry-Perot interferometers used on large fusion devices such as tokamaks is generally considered as a challenging task. In such devices, the ECE diagnostic is located tens meters away from the plasma chamber, which gives very low incident powers on detectors. Moreover, there are some specific difficulties associated with the use of Fabry-Perot interferometers by comparison with very well tested measurements obtained for example with Michelson interferometers. To compare these two types of spectrometers, it is usual to estimate the total integration time required for calibration. We have to consider the Michelson multiplex advantage compared with Fabry-Perots [7]. Let $\Delta t$ be the Michelson scanning time used to measure one spectrum over a total frequency bandwidth $\Delta f$. If $\delta f$ is the Fabry-Perot frequency resolution with $\frac{\Delta f}{\delta f} = M_e$ , every $\delta f$ is only observed during $\frac{\Delta t}{M_e}$ with a Fabry-Perot interferometer. The same signal-to-noise ratio would then be obtained for an integration time $M_e$ times longer in the latter case. Typically, if Michelson calibration has been achieved in 10 hours, with a multiplex factor estimated to 30, one would calibrate Fabry-Perot instruments in 300 hours ! The second difficulty arises when one has to measure DC levels during very long integration times. Third, intrinsic to the Fabry-Perot interferometer is the problem of rejecting the high order transmission of the cavity. The high frequencies of the *étalon* (black body) source spectrum must be properly filtered with particular attention to the $\omega^2$ dependence of the black body law.

To quantify what kind of signals are involved in such measurements, we recall that the typical signal during standard operation on the Tore Supra tokamak is in the range of 100 nW associated with 0.1 mV signal on the detector (detector detectivity close to 1000 $VW^{-1}$). Standard black body sources used to calibrate ECE diagnostic *in situ* are 3 $10^4$ times colder. They involve powers close to 3 pW with 3 nV voltage to be detected. A convenient calibration technique should be able to detect 0.1nV signal and thus to discriminate signal-to-noise ratio as low as $10^{-5}$ since the typical input noise is of the order of 0.01 mV. Actually, for a given detector NEP, namely 1.5 $10^{-13}$ $WHz^{-1/2}$ in our case, the minimum detectable power before processing is related to the frequency bandwidth of the detection technique. A convenient correlation technique has then to be used in order to increase the signal-to-noise ratio as necessary.

The power levels involved in calibration of Fabry-Perot interferometers used on large tokamaks are generally not compatible with usual data processing techniques such as coherent addition or synchronous detection [8,9]. We present in this paper a new method able to detect DC signals as low as 0.1 nV. It is based on a correlation technique used to increase the output signal-to-noise ratio $R_0$ together with a proper reduction of the detection frequency bandwidth introduced to optimize the input signal-to-noise ratio $R_i$. The principle of this method is the following : the source signal is chopped and coherently added over M turns of the chopper. The resulting signal is Fourier analysed and one finally takes the amplitude at the chopper frequency, which gives an ideal filtering of noise. Incident powers less than 1 pW have thus been measured.

Until now and probably due to the difficulties detailed above, absolute calibration of Fabry-Perot interferometers has not yet been achieved for applications to plasma diagnostics in large fusion devices [10]. Usually, these measurements are calibrated relatively to other diagnostics such as, for example, Thomson scattering or Michelson spectrometers. The method presented is the first developed which has achieved this goal. Of course, this method could be used in a more general context every time DC signals with signal-to-noise ratios less than $10^{-5}$ have to be measured.

The experimental set up is briefly described in Sec.II. Then, we detail the method and its performance (Sec.III). We present the resulting plasma temperature and validate the new method in calibrating a Michelson interferometer in Sec IV. Last, some further points related to correlation techniques will be discussed (Sec.V).

## II. EXPERIMENTAL SET UP

On Tore Supra [11] as well as on other large tokamak devices, the ECE interferometers are located far away from the plasma [12]. Each optical coupling line, 35 m long, is made of oversized ( 50 mm ) circular waveguides and 9 bends. InSb semi-conductors cooled in a cryostat at liquid Helium temperature are used as quantic detectors. They convert the incident electromagnetic radiation ( typically $\approx 10^{-7}$ Watt for 10 GHz spectral bandwith during standard plasma operation ) into voltage signal ( typically $\approx 10^{-4}$ V ). This signal has to be compared to the measured input noise $\approx 10^{-5}$ V which gives an input signal-to-noise ratio $R_i \approx 10$.

The calibration source is an extended area ( 20 x 20 cm ) black body source with a high degree of uniformity and precision temperature control ($\pm$ 2° up to 600° C ). The emissivity is very close to 1 ( > .87 ) in the submillimeter wavelength region ( 100 - 1000 GHz ). The maximum effective temperature is then slightly above 800 K which is 4 or 5 orders of magnitude below the standard plasma temperature. In these conditions, the expected output detector signal ( $10^{-9}$ V ) is far below the thermal noise amplitude and the input signal-to-noise ratio becomes $R_i \approx 10^{-4}$ . The successful calibration is actually determined by the ability to adequately increase the output signal-to-noise ratio $R_o$ of the measurement.

A schematic of the calibration line is given in Fig.1. In order to minimize the systematic error in calibation, we installed the *étalon* source in situ, at the plasma location. The black body intensity is first modulated by a 30 cm diameter chopper at a frequency of 280 Hz. For every turn of the chopper, an incremental encoder delivers 1 synchronisation pulse and 512 TTL pulses used as an external clock to trigger the data acquisition.

The Fabry-Perot cavity is composed of two reflecting meshes as usual in the far infrared domain. The moving grid is mounted on a step-by-step translation table ( each step : 2.5 $\mu$m ) monitored by a micro-computer. Rejection of higher order transmission of the cavity is achieved replacing mirrors by reflection gratings in the line bends.The cut-off frequency, depending on the grating constant ( .7 and .8 mm ) is approximately 300 GHz. Numerical simulation taking into account , i) the $\omega^2$ dependence in the black body radiation law, ii) the drastic decrease of the cavity finesse with frequency ($\alpha\ \omega^{-2}$), iii) the individual response of each optical components such as antenna with fused quartz window, waveguides, bends, polarizer, grating filters ... etc, indicated that

4 reflection filters were necessary in order to recover a measured spectrum equal to the expected spectrum within 5 % error bars.

The voltage detector signal is amplified by a very low noise amplifier switched on AC position during calibration procedure. Data acquisition is performed on INTEL modules with 2 RAMs 16 bit x 32 k. One RAM is loaded while the other is being read and stored by the CPU ( 80386 ). This allows continuous acquisition at a frequency up to 100 kHz without loss of data. Both the control unit and the data acquisition modules are Multibus compatible and installed in the same frame.

Real time data processing is performed (see Fig.2). This consists first in a coherent digital addition of the signal over M turns of the chopper for a given cavity spacing ( coherency is ensured by means of synchronization pulses ). After a delay as long as required to increase the output signal-to-noise ratio proportionally to $\sqrt{M}$, a sinusoid is obtained with the same number of period as the chopper holes number. The resulting sinusoid is centered on y-axis by using AC amplifiers. This sinusoid is then Fourier analysed ( 512 points ). As a final step, the 280 Hz amplitude in the frequency space is stored [13]. The same procedure is repeated for each spacing of the Fabry-Perot cavity in order to obtain the final calibration curve $C(\omega)$. The advantages of the Coherent Fourier Analysis ( CFA ) just described are reviewed in the following section.

## III. CFA PERFORMANCE

### A. Preliminaries

When such low signals are to be detected, two preliminary conditions must be fulfilled by the amplification chain in order to properly recover the amplitudes. They are related to the 12 bits A-D converter used to store the data. Starting with an input signal close to 1 nV, it is necessary for the output signal to have an amplitude greater than 1 bit of the converter, namely 4.88 mV in our case. This leads to a minimun value for the gain of the whole amplifying chain : $G_{min} \approx 5.\ 10^6$. Another consequence of using such converters is that the maximum output amplitude is limited to $\pm$ 10 V. Of course when using such voltage gains, the amplified noise could saturate the converter. It is then necessary to reduce the frequency bandwidth as close as possible to the frequency to be detected ( 280 Hz ) and to adjust the maximum gain in order to obtain an output signal less than 10 V. By

introducing an analog filter 100 - 500 Hz between the amplifiers and the acquisition module, we have determined $G_{max} = 10^7$.

**B. Gain in signal-to-noise ratio**

When coherently adding M samples of 512 data points for each turn of the 7-holes chopper, an exact 7-period sinusoid is recovered. The input signal can be written as :

$$x(t) = a_s + n(t)$$

where $a_s$ is the signal amplitude to be measured and n(t) the noise amplitude. Chopping the signal besides the source and centering by using an AC amplifier will produce (after normalization by the gain ) :

$$x(t) = \frac{a_s}{2} \sin( N_h \omega_c t + \phi_0 ) + n(t) \qquad \text{(III.1)}$$

in which $N_h$ is the chopper holes number, $\omega_c = \frac{2\pi}{T_c}$ is the chopper frequency, $T_c$ the chopper period and $\phi_0$ a possible phase difference due to the synchronisation pulse position. The coherent adding over M turns of the chopper will give, for the 512 $t_i$ points in the interval $[0,T_c]$ :

$$z(t_i) = \frac{a_s}{2} \sin( N_h \omega_c t_i + \phi_0 ) + \frac{1}{M} \sum_{k=0}^{M-1} n(t_i - kT_c) \qquad \text{(III.2)}$$

It is well known here that the average value $E\{z(t_i)\}$ of $z(t_i)$ equals the first term in (III.2) in the case where n(t) is centered. The variance of $z(t_i)$ defined as $E\{ |z(t_i) - E\{z(t_i)\}|^2 \}$ can be derived in order to calculate the output noise power. It writes :

$$\text{var} \{ z(t_i) \} = \frac{1}{M^2} \sum_{k=0}^{M-1} \sum_{l=0}^{M-1} C_{nn}((l-k)T_c)$$

in which $C_{nn}$ is the noise autocorrelation function . This latter expression can be written :

$$\text{var} \{ z(t_i) \} = \frac{1}{M^2} \sum_{k=0}^{M-1} C_{nn}(0) + \frac{2}{M} \sum_{k=1}^{M-1} (1 - \frac{k}{M}) C_{nn}(kT_c) \qquad \text{(III.3)}$$

We assume that the noise spectral density is constant and equal to $\frac{\sigma_n^2}{2 \nu_{max}}$ in a given frequency bandwith $[-\nu_{max}, +\nu_{max}]$ around the chopper frequency so that the total noise power is $\sigma_n^2$. We have verified that the noise autocorrelation function vanishes rapidly in time so that $C_{nn}(T_c) \approx 0$. Hence, one recovers the standard result :

$$\text{var} \{ z(t_i) \} = \frac{\sigma_n^2}{M}$$

which shows that, starting with an input signal-to-noise ratio $R_i = \frac{a_s}{\sigma_n}$, the output signal-to-noise ratio becomes after averaging (and normalized to the gain of the amplifying chain) :

$$R_o = \frac{a_s \sqrt{M}}{2 \sigma_n}$$

Now, let us quantify what is the effect of the discrete Fourier transform on $R_o$. Let $T_c$ be the chopper period ( $\frac{1}{T_c}$ = 40 Hz ) and $N_{DFT}$ = 512, the number of data points per turn. The sampling frequency is $\nu_s = \frac{N_{DFT}}{T_c}$ = 20.5 kHz. In order to avoid spectrum alliasing, the input signal at a maximum frequency given by $\nu_{max} = \frac{\nu_s}{2}$ = 10.25 kHz has to be filtered . Taking $N_{DFT}$ points between 0 and 2 $\nu_{max}$, the discrete Fourier transform samples the spectrum every $\delta\nu = \frac{2\nu_{max}}{N_{DFT}} = \frac{1}{T_c}$ = 40 Hz. At this point, there is an interesting property of the discrete Fourier transform : Taking into account the sinusoid is $T_c$-windowed in time , the $\frac{\sin(\pi T_c \nu)}{2\pi\nu}$ convolution in frequency space produces secondary lobes with a periodicity just equal to the sampling interval $\delta\nu = \frac{1}{T_c}$ . In these conditions, the secondary lobes just cancel. As a consequence, the total power of the chopping frequency ( 280 Hz ) is recovered in the $(N_h + 1)^{th}$ point of the discrete Fourier transform ( the number $N_h$ is due to the exact $N_h$ period sinusoid in time space ). For this reason, the total input noise power initially equal to $C_{nn}(0) = \sigma_n^2$ will reduce to $C_{nn}(0)\frac{\delta\nu}{2\,\nu_{max}} = \frac{\sigma_n^2}{N_{DFT}}$ .

If $a_f$ is the amplitude of the $(N_h + 1)^{th}$ point of the DFT and $\mathbf{K} = \frac{a_s}{a_f}$, the conversion factor to be determined in order to deduce $a_s$ (see next paragraph), $R_o$ becomes $R_o = \frac{\mathbf{K}\, a_f \sqrt{N_{DFT}}}{2\,\sigma_n}$ hence :

$$R_o = \frac{\sqrt{N_{DFT}\, M}}{2} R_i \qquad \text{(III.4)}$$

It is important to notice that $R_o$ cannot be adjusted as wanted by increasing $N_{DFT}$. Of course, as previously seen, $N_{DFT}$ and the maximum frequency in the spectrum are related by $\frac{2\nu_{max}}{N_{DFT}} = \frac{1}{T_c}$ (so that $R_i$ decreases as $N_{DFT}$ increases). The quality factor $N_{DFT}$ just exhibits the ability of the numerical filtering to take one frequency point in a given noise bandwidth.

To summarize, starting with a signal amplitude $a_s$ "drowned" in noise (due to detectors, electronics thermal noise and any background noise), one obtains an amplitude $a_f$ in Fourier space that corresponds to the amplitude of the peak at the chopping frequency. To properly reconstruct the real amplitudes, one has to determine now the conversion factor $\frac{a_s}{a_f}$ introduced by CFA. This is detailed hereafter.

### C. Determination of the CFA conversion factor

For a given sinusoid amplitude $a_s$ associated with the black body chopped signal, the final amplitude $a_f$ given by the CFA must be evaluated ( in order to deduce $a_s$ when measuring $a_f$ in the calibration procedure ).This conversion factor **K** has a mathematical and mechanical origin only. It

depends both on the numerical method used to convert $a_s$ in $a_f$ ( discrete Fourier transform ) and on the mechanical coupling between the black body and the chopper ( generating a more or less pure sinusoid ). It can be experimentally evaluated measuring the ratio $\frac{a_s}{a_f} = K$ when the sinusoid is visible. For this reason, we removed the grid from the Fabry-Perot cavity and could determine $a_s$. The conversion factor deduced is equal to $\frac{1}{123}$ . Taking 512 points for the discrete Fourier transform gives a conversion factor equal to $2(\frac{2}{512}) = \frac{1}{128}$ .This correspond to the theoretical value of the mathematical transform only ( the first factor 2 is due to the duplication of peaks in the discrete Fourier transform and the second one is due to the initial amplitude being equal to $\frac{a_s}{2}$ ).

## IV. RESULTS

### A. Fabry Perot calibration

The automation of the calibration procedure ( programmable cavity spacing control and continuous data acquisition and processing ) allowed us to start a long duration calibration ( a week-end for example ) without necessity of any human presence. Fig. 3a represents an example of the coherent sinusoid obtained after an integration time of 16 mn for a cavity spacing corresponding to 220 GHz and Fig.3b, the associated discrete Fourier transform. The intensity of the peak together with the help of the conversion factor, implies a measured input voltage of 1.55 nV. Fig.4 shows the final spectrum obtained for 80 different cavity spacing between 175 and 325 GHz with an integration time of 52 mn per point. The total calibration time, free of any electrical interferences and mechanical vibrations has been 70 hours for one Fabry-Perot line. One recognizes the $\omega^2$ dependence in the low frequency part of the spectrum. The sharp decrease around 300 GHz is due to the 4 reflection gratings used as low-pass filters.

Application to plasma measurements and comparison with two other independent absolute $T_e$ measurements are given in Fig.5. It appears that the agreement is quite good. New calibrations performed recently indicated an excellent reproductibility of the calibration spectrum both in shape and amplitude.

## B. Testing CFA on Michelson calibration

A way to assess the advantages of the CFA method is to compare the calibration of a Michelson interferometer using first the standard coherent addition technique and then, the detection technique described in this paper. To achieve this, one of the two mirrors (#1) in the interferometer arm has been mounted on a vibrator while the second one (#2) has been installed on a step-by-step translation table. During coherent addition, interferograms of $N_p = 400$ points are added over $M_{CA}$ periods $T_v$ of the vibrator, mirror #2 remaining fixed. During CFA, mirror #1 is fixed. For each one of the 400 positions of mirror #2, the signal is processed over $M_{CFA}$ periods $T_c$ of the chopper. The total integration time is then :

$$t_{CA} = M_{CA}\, T_v \qquad \text{(IV.1)}$$

for the standard correlation technique and :

$$t_{CFA} = N_p\, M_{CFA}\, T_c \qquad \text{(IV.2)}$$

for the CFA technique. Taking $T_v$ of the order of $T_c$ in our experiment, it appears that the total integration time after the same number of samples is $N_p$ times longer using CFA.

Now, let us come back to the resulting signal-to-noise ratio $R_o$ as a function of the total number of samples added, using the two techniques. In both cases, $R_o$ is estimated taking the peak-to-peak intensity of the interferogram near (signal) with respect to far from (noise) the central fringe. We have plotted in Fig.6 the output signal-to-noise ratio obtained in function of the number M of samples added. The solid lines correspond to analytical fits proportional to $\sqrt{M}$ .According to equation (III.4), one would expect a multiplying factor of $\sqrt{512}$ between the two methods since in standard coherent addition, one has :

$$R_o = \sqrt{M_{CA}}\, R_i \qquad \text{(IV.3)}$$

This would be true if we started with the same $R_i$ in the two methods. This is not our case since the frequency bandwidths are respectively $\Delta B^{CFA}$ = 100-1000 Hz and $\Delta B^{CA}$ = 30 kHz in CFA and coherent addition. It is easy to show that :

$$\frac{R_i^{CFA}}{R_i^{CA}} = \sqrt{\frac{\Delta B^{CA}}{\Delta B^{CFA}}} \qquad \text{(IV.4)}$$

hence :

$$R_o^{CFA} = \frac{\sqrt{N_{DFT}}}{2} \sqrt{\frac{\Delta B^{CA}}{\Delta B^{CFA}}}\, R_o^{CA} \qquad \text{(IV.5)}$$

A numerical estimation gives $R_0^{CFA} = 65\ R_0^{CA}$ . It appears from Fig.6 that $R_0^{CFA}$ (left curve) $\approx 14.8\ R_0^{CA}$ (right curve) . This apparent discrepancy is due to a bad optimization between numerical and analogical filtering. It will be discussed in more detail in the next paragraph.

We are now able to evaluate the expected integration time needed to obtain the same $R_0$ in both cases. By using equations (III.4) , (IV.1), (IV.2) ,(IV.3) and (IV.5), we find :

$$t_{CFA} = \frac{N_p}{N_{DFT}} \frac{\Delta B^{CFA}}{\Delta B^{CA}} \frac{T_c}{T_v}\ t_{CA} \qquad \text{(IV.6)}$$

which shows that CFA obtains better results than usual correlation techniques since $N_p = 400$, $N_{DFT} = 512$ , $\frac{\Delta B^{CFA}}{\Delta B^{CA}} < 1$ and $T_c \approx T_v$. As a final comparison, we represent in Fig. 7 the calibration interferograms obtained with the two methods after a total number of samples equal to 8000 in both cases.

## V. DISCUSSION

Two main methods have been developed to increase signal-to-noise ratios : the well known coherent addition and synchronous detection. Before having obtained good results with CFA, we tried first to use these methods. Difficulties encountered and some additional points are discussed in this section.

In the first case, we controlled the moving grid of the Fabry-Perot cavity in order to scan the total spectrum ( 175 - 325 GHz ) and coherently added M spectra as in the Michelson calibration procedure. Using programmable stepping motors ( 1 step : 2.5 μm ; maximum speed : 40 kHz ), it was possible to reach a scanning frequency of 20 Hz. Amplifiers were used in DC position as is the case during plasma measurements. This procedure, which increases the signal-to-noise ratio as $\sqrt{M}$, failed mainly for two reasons. First, electronical DC drifts and offsets up to 10 nV per second are sufficient to mask the black body signal. Second, a very intensive background signal attributed to external power falling directly in the Fabry-Perot cavity has been observed. Even installing the black body source in the vicinity of the Fabry-Perot and substracting the signal when the source is removed, the resulting signal is only 5 % of the total power. If placed in situ, the black body contribution should become negligible and thus the method has been abandoned.

A way to eliminate this background level consists in chopping the incident power using, for instance, synchronous detection. The Fabry-Perot cavity is then operated in static mode, i.e fixed spacing, and the amplifiers are switched on AC position. An analogical bandpass filter is used for the detection around the chopping frequency. Actually, limitation on integration time in lock-in amplifiers does limit the maximum gain in signal-to-noise ratio. In practice, this limit is close to $10^5$ whereas $10^6$ is required in our case. The method, successfully tested when the black body is in the Fabry-Perot vicinity, is inadequate when placing the source in situ, 30 m away. Moreover, uncertainties due to both lock-in voltage gain and manual adjustment of the reference signal result in additional uncertainties for accurate measurements of absolute signals.

On the contrary, the dynamic range in Coherent Fourier Analysis is ultimately limited by fixed ( not random ) errors. These are only due to the uncertainty in the temperature of the calibration source (< 0.5%) and to the systematic error introduced by the determination of the conversion factor (estimated less than 1%). The gain in signal-to-noise ratio is mainly limited by the time devoted to the calibration. In the laboratory, we have measured the reproductibility of the method as a function of the total number of points coherently added i.e, as a function of time. Fig.8 shows the dispersion in the resulting amplitude at 220 GHz as a function of the total number of samples. The optical line was nearly the same as the Tore Supra line, in order to measure very low signals as well. The figure shows the good convergency of the method. By starting a new acquisition when the source has been removed, we have verified that the background noise spectrum effectively cancelled in time.

CFA combines the advantages of the two previous methods. Coherent addition is first used to increase the signal-to-noise ratio as required while chopping the input power and so using AC amplifiers eliminates both electronical drifts, offsets and the background ( un-chopped ) signal. Finally, Fourier analysis provides an ideal signal filtering, which increases the resulting signal-to-noise ratio.

Coming back to equation (IV.5), it is important to correctly combine analog and numerical filtering. Indeed, as we have seen before, the sampling frequency $\nu_s = \frac{N_{DFT}}{T_c}$ is determined by the number of points taken in the discrete Fourier transform. When $N_{DFT} = 512$, we have noticed in § III.B that the input signal should be filtered to a maximum value $\nu_{max} = 10.25$ kHz. This is 10 times the real value (100 - 1000 Hz) chosen in order to avoid the saturation of output converters. This

means that $N_{DFT}$ could be reduced to 64 without loss of information. In the latter case, equation (IV.5) gives $R_o^{CFA} = 20\, R_o^{CA}$ which is now compatible with the measurement (Fig.6). This proves that analog and numerical filtering must be consistent to give the best results (reducing $N_{DFT}$ allows increase of the chopper frequency for a given sampling frequency, which thus increases the number of samples M).

Using equation (IV.6), the CFA time saving with respect to coherent addition is depending on the factor :

$$g = \frac{N_{DFT}}{N_p} \frac{T_v}{T_c} \frac{\Delta B^{CA}}{\Delta B^{CFA}}$$

Starting with the same input signal-to-noise ratio Ri for the two methods, application to the Fabry-Perot calibration time gives $g \approx 5$ , taking the scanning period of the Fabry-Perot cavity $T_v \approx T_c$, the number of frequency points in the spectrum $N_p = 80$ and $N_{DFT}$ adapted to the analogical filtering. This result is compatible with the effective calibration time (65 hours), compared to what was expected by using the standard coherent addition (300 hours).

As an additional remark, one may notice that the method provide no error induced by random or systematic drift in the frequency of the chopping system. The resulting 7 period sinusoid is independent of the chopper frequency since the number of data points per turn remains fixed. The chopper frequency around 40 Hz can vary slowly in time during the calibration. The information is always avalaible in the $(N_h + 1)^{th}$ point of the discrete Fourier spectrum.

We finally applied the procedure in order to check for the linearity of the detectors for very low temperature sources. Fig.9 shows the final result after an integration time of 35 hours ( corresponding to $5.6\ 10^6$ points ) in function of the source temperature. The minimum measured amplitude corresponding to the 150°C is 0.4 nV.

## VI. CONCLUSION

We have developed in this paper a method (named CFA for Coherent Fourier Analysis) based on a correlation technique and optimized signal filtering which can be used to detect DC signals when the input signal-to-noise ratio is less than $10^{-5}$ . It has been shown how the coherent addition of the chopped signal sampled $N_{DFT}$ times during the chopper period (with $N_{DFT}$ equal to a power of 2) leads to a final amplitude $a_f$ in Fourier space proportional to the signal amplitude $a_s$ to be measured.

The right signal amplitude is then deduced from a conversion factor that can be easily determined. The resulting gain in signal-to-noise amplitude ratio is $\frac{\sqrt{N_{DFT}}}{2}$ with respect to standard averaging methods. On the other hand, the total integration time needed to obtain a given output signal-to-noise ratio has proved to depend on the factor $\frac{N_{DFT}}{N_p}\frac{T_v}{T_c}$ where $N_p$ is the total number of points in the spectrum, $T_v$, the vibrator scanning period used in the averaging method and $T_c$, the chopper period introduced in CFA (the factor $\frac{\Delta B^{CA}}{\Delta B^{CFA}}$ appearing in equation (IV.6) has just been introduced to normalize the input noise powers). The principal advantage of the CFA method is the possibility to reduce the frequency bandwidth as close as possible to the chopping frequency without distortion of the signal. Doing this, it is necessary to adjust $N_{DFT}$ in order to optimize the correlation. In standard averaging methods, this frequency bandwidth cannot be significantly reduced in order to reconstruct the real shape of the signal during the scan. Moreover, the method provides virtually unlimited gain in signal-to-noise ratios. The accuracy of the measurement is just limited by the systematic error induced by the method which has been estimated to 1%.

This method has been successfuly tested in calibrating a Fabry-Perot interferometer used on a large tokamak (Tore Supra) in order to measure the absolute electron temperature of the plasma. It has also been applied to the Michelson calibration. Signals as small as 0.4 nV have been measured.

## REFERENCES


/1/ J.M.VAUGHAN, *The Fabry-Perot interferometer*, Adam Hilger, Bristol & Philadelphia, 1989.

/2/ G.W.CHANTRY, *Submillimetric spectroscopy* , Academic Press, London & New-York, 1971.

/3/ E.A.M.BAKER , B.WALKER , *Fabry-Perot interferometers for use at submillimetre wavelengths* , J.Phys.E : Sci. Instrum 15, 1982.

/4/ F.ENGELMAN, M.CURATOLO, Nucl. Fus. 13, 497, 1973.

/5/ A.E.COSTLEY, R.J.HASTIE, J.W.M.PAUL AND J.CHAMBERLAIN, *ECE from tokamaks : Experiment and theory* , PRL, 33, (758), 1974.

/6/ B.WALKER, E.A.M.BAKER and A.E.COSTLEY, *A Fabry-Perot interferometer for plasma diagnostics,* J.Phys.E : Sci. Instrum 14, 1981.

/7/ R.J.BELL, *Introductory Fourier transform spectroscopy* , Academic Press, Inc, 1972.

/8/ J.MAX, *Methodes et techniques de traitement du signal* , T1 & 2 Masson, 1985 & 1987.

/9/ A.PAPOULIS, *Probability, Random variables and stochastic processes* , M$^{c}$ Graw Hill, 1984.

/10/ C.JAVON, Ph.D Thesis, Paris 6, 1991.

/11/ Equipe TORE SUPRA presented by R.AYMAR, *First experiments in Tore Supra* , in 12$^{th}$ IAEA conf. on plasma physics and controlled nuclear fusion , Nice, 1988.

/12/ L.LAURENT, L.RODRIGUEZ and M.TALVARD, *ECE diagnostic on Tore Supra,* in Controlled fusion and plasma heating 11D, III, 1304, (14$^{th}$ EPS), Madrid, 1987.

/13/ C.JAVON, M.TALVARD , *Calibration of Fabry Perot interferometers for ECE measurements on the Tore Supra tokamak,* in 15$^{th}$ int'l conf. on infrared and mm waves, Orlando, USA, 1990.

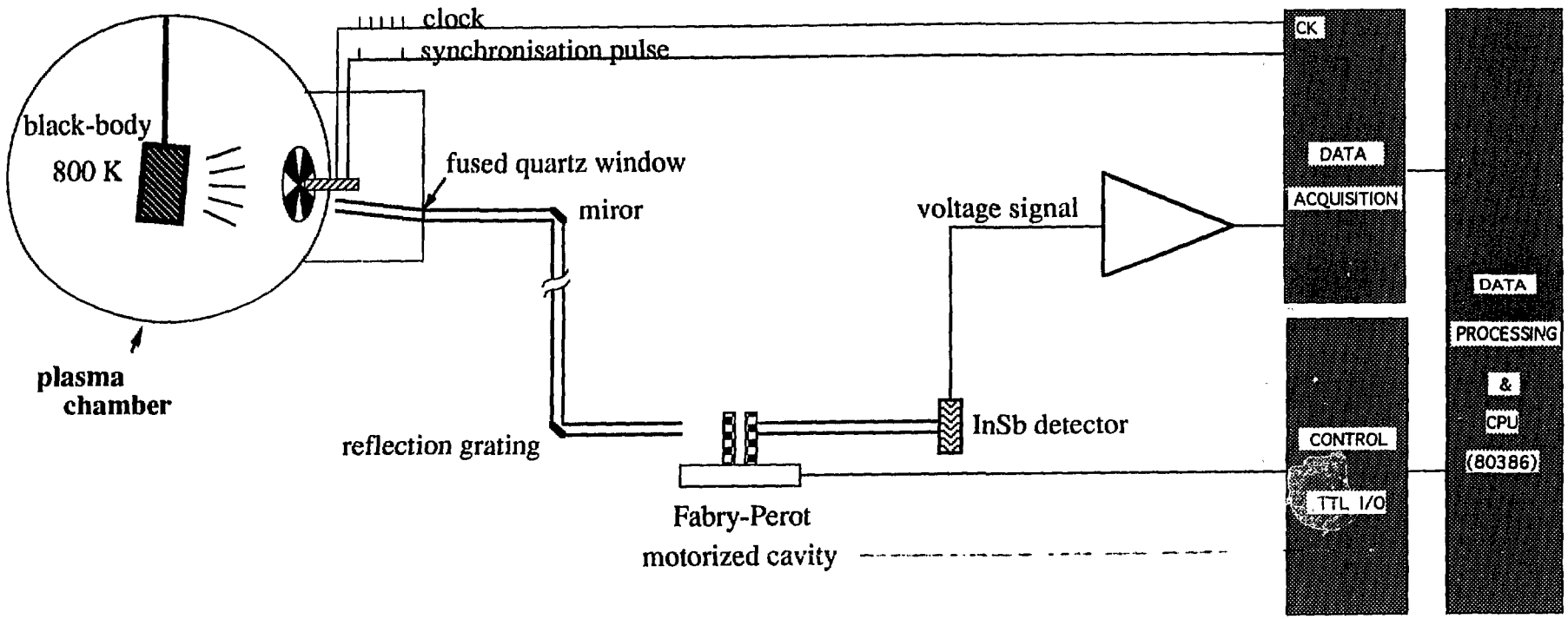


Fig.1 Calibration set up

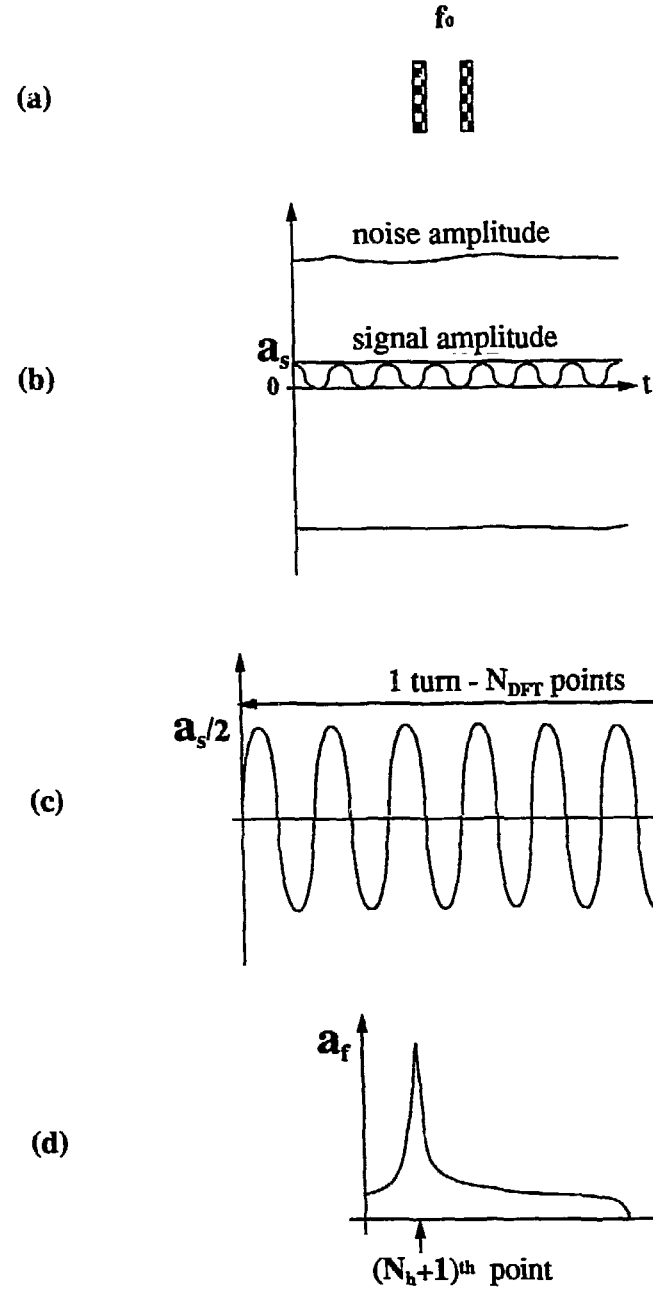


Fig.2 Principle of Coherent Fourier Analysis
(a) Taking 1 Fabry-Perot cavity spacing.
(b) Chopping the signal besides the source.
(c) Coherent adding over M chopper turns & AC amplifying.
(d) Discrete Fourier Transform of (c).
(e) Storing the $(N_h+1)^{th}$ point of DFT $(a_f)$.

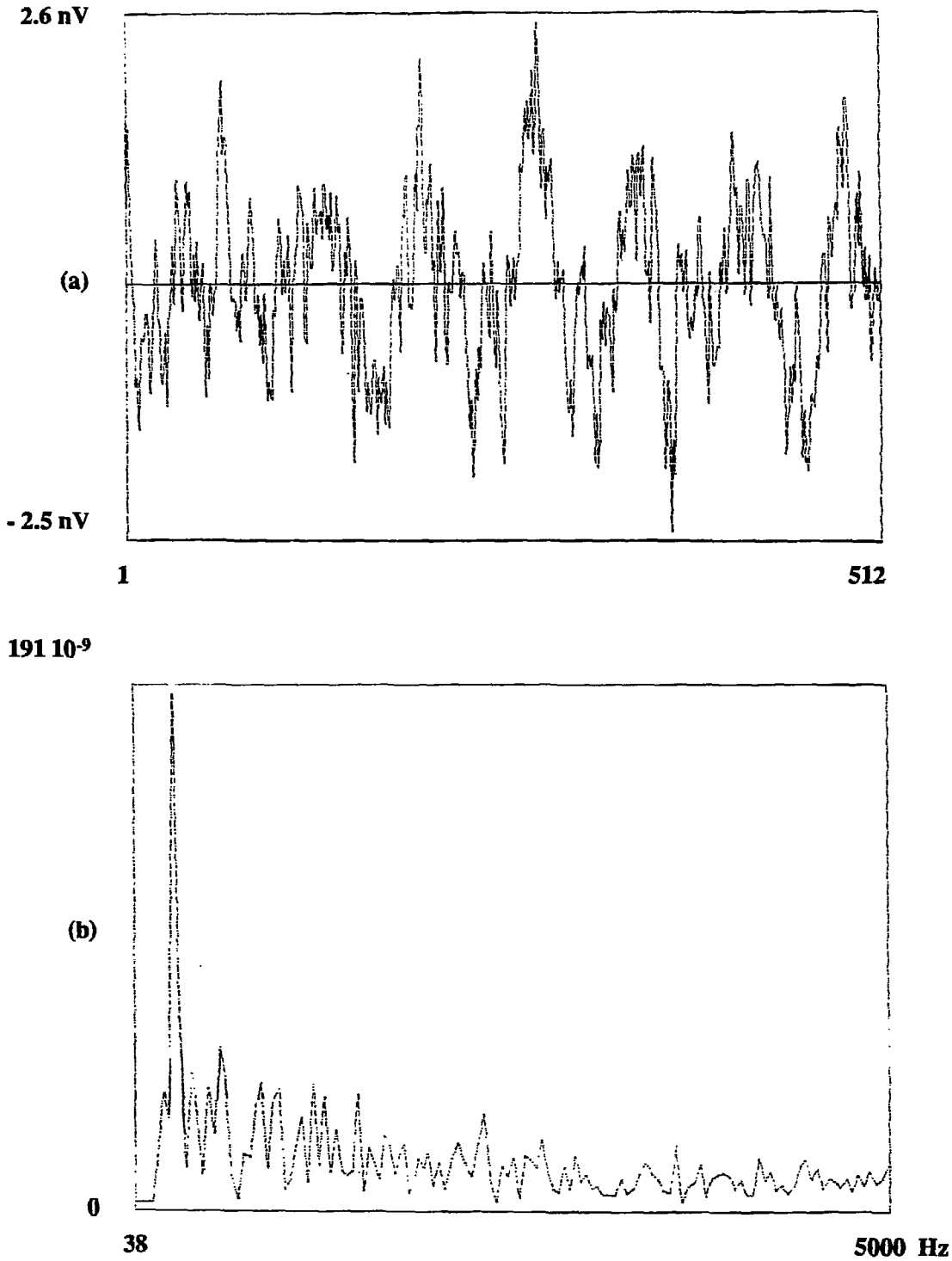


Fig.3 (a) Signal correlation during 16 mn
(40000 turns - 1 cavity spacing).
(b) Discrete Fourier transform of (a).

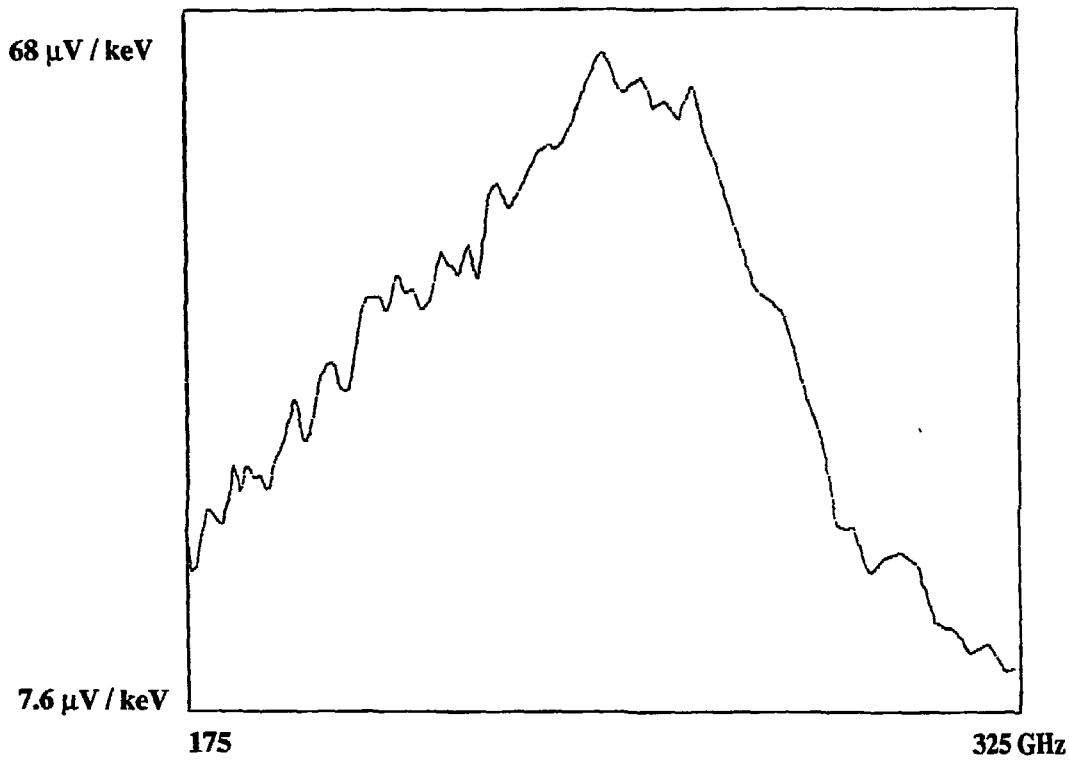


Fig.4 Calibration spectrum
( 80 frequency points - 50 mn integration time per point )

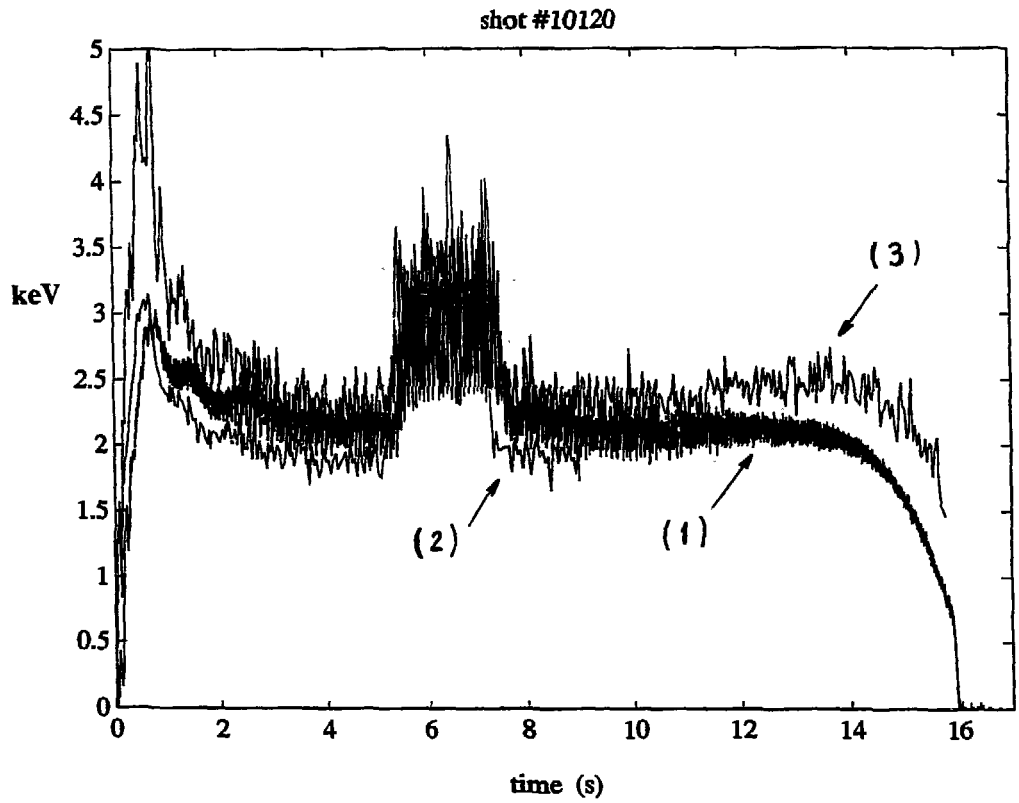


Fig.5 Absolute $T_e$ measurement from Fabry-Perot (1), Michelson interferometry (2) and Thomson scattering (3).

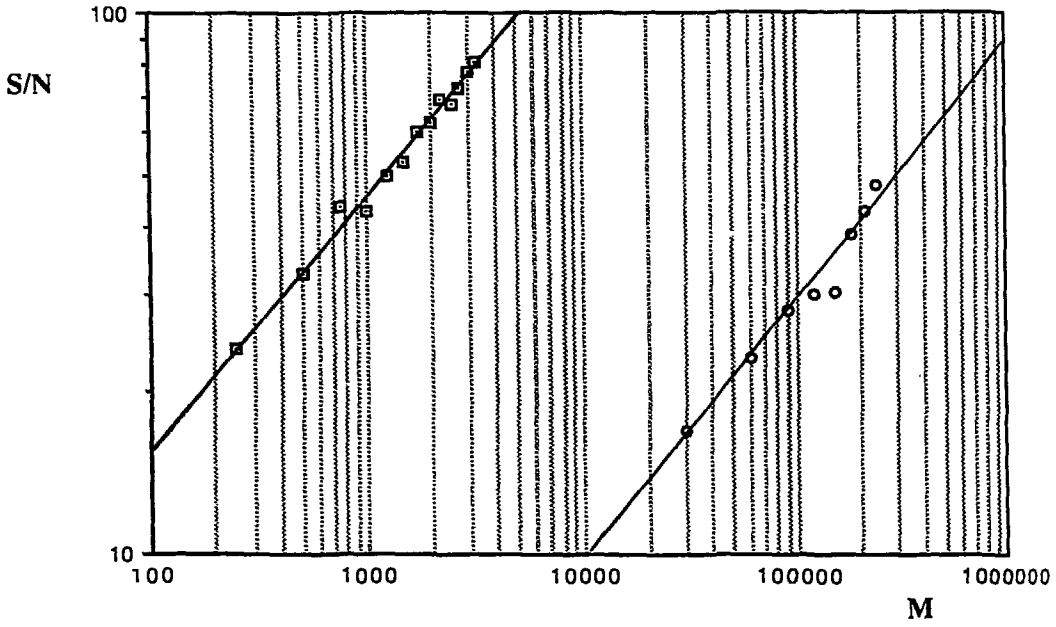


Fig.6 Comparison of the resulting signal-to-noise ratios using Coherent Addition (circles) and CFA (squares).

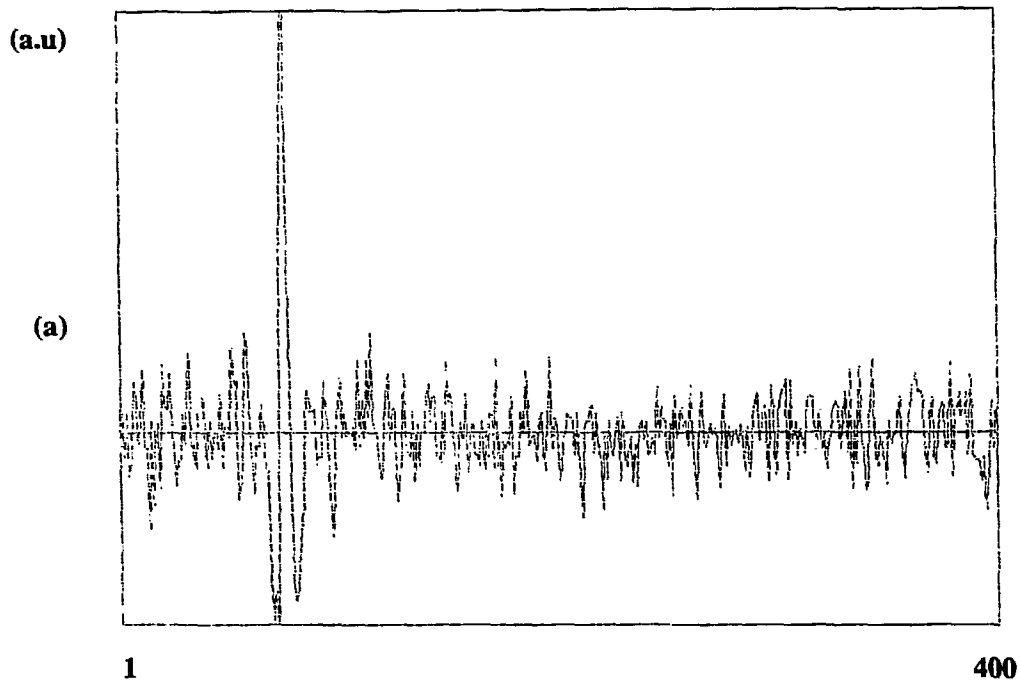


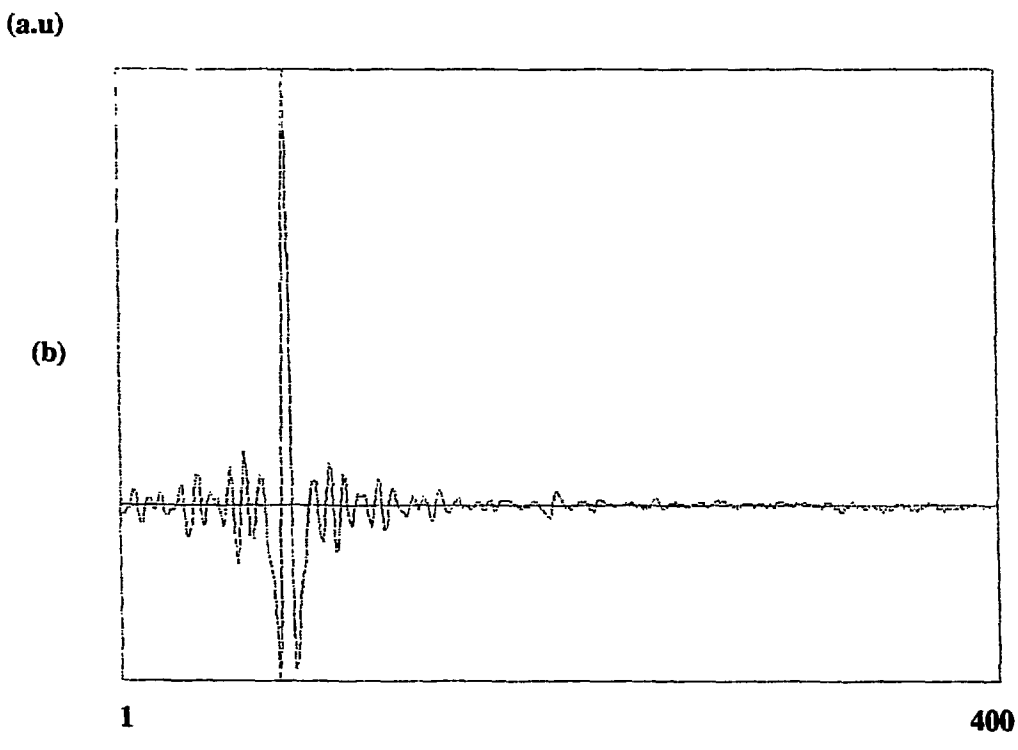


Fig.7 Michelson calibration interferograms using a standard correlation method (a) and CFA (b) , for 8000 samples in both cases.

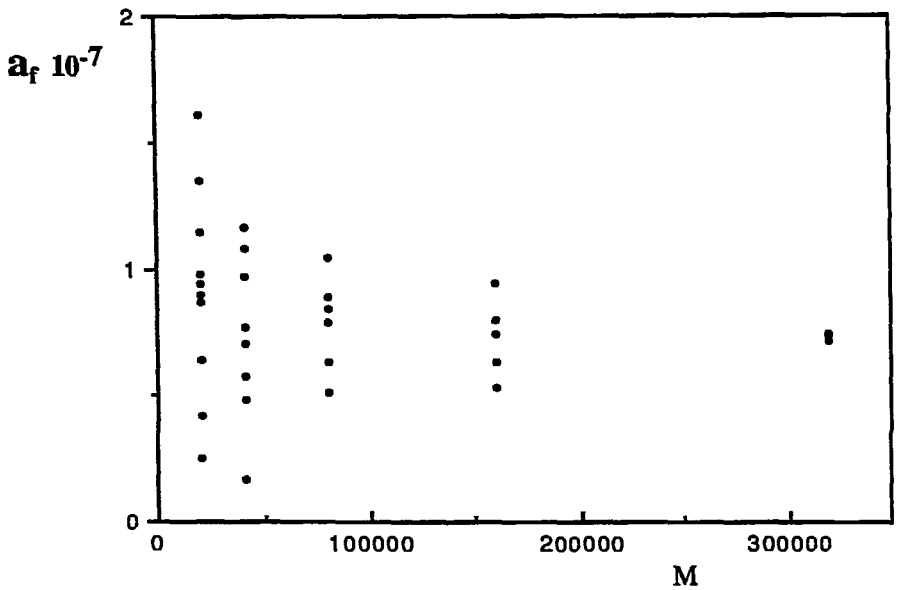


Fig.8 Dispersion of CFA output amplitudes.
( 100000 turns = 40 mn )

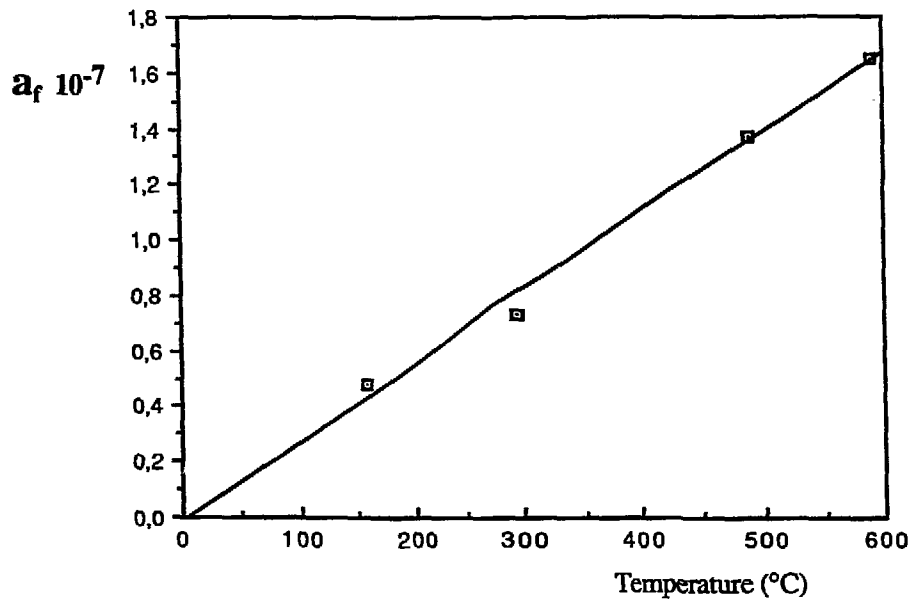


Fig.9 Check for linearity of detectors